IEEE Trans. Circuits & Systems Part 1, published online November 2008

Preferred Transmission Frequency for Size-Constrained Ultralow-Power Short-Range CMOS Oscillator Transmitters

David C. Yates, *Member, IEEE,* and Andrew S. Holmes, *Member, IEEE*

***Abstract*— A method is presented for minimising the power consumption of size-constrained oscillator transmitters by selecting the preferred carrier frequency from among the standard ISM bands. The method has been applied to CMOS oscillator transmitters in which a single turn loop antenna doubles as the inductor in the frequency-defining LC tank. A detailed model of the transmitter circuit, including the antenna, is combined with standard assumptions about the link and receiver to determine the minimum transmitter bias current for successful demodulation as a function of antenna size and transmission frequency. From this the optimal operating frequency in terms of transmitter power budget, and the minimum transmitter power consumption at that optimal frequency, are determined for a given antenna size constraint. Two common oscillator topologies are studied, both implemented in 0.18 μm CMOS: the Colpitts oscillator and the complimentary cross-coupled oscillator. A combination of the EKV and BSIM models is used for MOS transistor modelling, while a novel energy conservation method is used to determine the oscillator bias current as a function of transmit power. The results show that, with the correct choice of operating frequency, transmitter power budgets of the order of 10 μW should be achievable for very short range (ca 1 m) radio links with data rates up to 1 Mb/s and antenna sizes down to several mm radius.**

***Index Terms*— LC oscillators, loop antenna, MOS transistor modelling, oscillator transmitters, ultralow power, wireless transmitter, wireless health monitoring.**

I. Introduction

Recent years have seen intense research in the area of wireless body area networks (BAN), aimed particularly at healthcare applications [1]. The development of wearable and implantable devices for monitoring and treating those suffering from chronic illnesses such as diabetes, heart disease and neurological conditions is following the rapid advancement in diverse areas such as MEMS technology, biomedical sensing, biocompatibility, low power electronics and energy scavenging [1]. Key to the realisation of these body sensors is the development of an ultra-low power miniature wireless transceiver [2].

Since BANs are limited to a range of only a few feet the output transmit power for each sensor node can be very low (sub-μW levels). At such low transmit powers it should be feasible to reduce each sensor's power budget for wireless communications down to the μW level where it will no longer dominate over that of the sensor electronics. This opens up the attractive possibility of wearable or implantable wireless sensors that can run continuously for years on a single coin cell. Power consumption in the μW range is also compatible with all types of energy harvesting power generator, including those based on MEMS technology [3].

A power budget of several μW is three orders of magnitude below what can be achieved by current commercial wireless solutions even at low (kb/s) data rates. Such a drastic reduction in power will probably only be achieved by adopting a hierarchical network topology where the transceiver in each sensor is reduced to bare minimum complexity, and all network configuration and control functions are handled by a smaller number of higher level network nodes. This might mean, for example, eliminating the frequency control elements that are normally associated with traditional transceiver designs, and instead having the sensors tune themselves to a reference signal from the higher level node prior to each transmission.

Recognizing the need for simplified transceivers, a number of groups have in recent years revisited traditional circuit topologies such as the oscillator transmitter [4]–[6] and the super-regenerative receiver [7], [8]. In an oscillator transmitter, a loop antenna is used as the inductive element in an LC resonator that defines the carrier frequency. A power amplifier is unnecessary due to the short transmission range. With a basic circuit topology such as the Colpitts oscillator, a very simple, short-range transmitter can be implemented with just a single off-chip inductor (the antenna), potentially giving very low circuit losses. Using on-off keying (OOK) the power consumption can be further reduced since the transmitter can be off for approximately half the time [4], [9]. The feasibility of this approach has been clearly demonstrated in several publications. For example, the link in [4] achieved a data rate of 1 Mb/s over 1 m range with an overall transmitter power consumption of only 300 μW. However, none of the work to date has addressed the problem of optimising the overall link design for minimum transmitter power consumption, and consequently all of the systems demonstrated have been sub-optimal in this respect.

A key challenge in the design of wireless transceivers suitable for on-body applications is the stringent constraint on antenna size. The trade-off between antenna efficiency and circuit losses, both of which increase with frequency, must be

Manuscript received September 4, 2007; revised April 15, 2008. This work was supported by the U.K. Engineering and Physical Sciences Research Council.

The authors are with the Department of Electrical and Electronic Engineering, Imperial College London, Exhibition Road, London SW7 2AZ, U.K. (email: david.yates@imperial.ac.uk; a.holmes@imperial.ac.uk)

carefully considered to achieve an ultra-low power solution. In this work we present a method of choosing the preferred transmission frequency from the standard ISM bands, given a constraint on antenna size, for the oscillator transmitter using a single turn loop antenna as the inductor in the LC tank.

Detailed analysis of the single-turn loop antenna, previously carried out by the authors, yielded a very important result, namely that the electrical size (i.e. circumference to wavelength ratio) of the antenna can be chosen such that both the radiation efficiency and the Q factor are high [10]. The single-turn loop is thus particularly suited to functioning as both antenna and tank inductor. In this paper we consider two oscillator topologies employing single-turn loops: the Colpitts oscillator and the complementary cross-coupled differential oscillator. These two topologies are chosen because they can both be implemented using a single inductor.

For a given oscillator topology and CMOS technology, the inputs to the optimisation process are the link transmission distance and data rate, the receiver noise figure and the allowed bit error rate. OOK modulation is assumed throughout, the transmission medium is air and the receiving antenna is taken to be a loop with an electrical size equal to 0.4 wavelengths, since this is optimal for a mobile size-unconstrained loop antenna. Both antennas are circular single-turn copper wire loops in air. The outputs are the preferred transmission frequency, chosen from among the ISM bands 434 MHz, 900 MHz, 2.45 GHz and 5.8 GHz, and the minimum transmitter bias current required for successful demodulation at that frequency, both expressed as a function of the transmitter antenna size. The optimisation procedure, implemented in MATLAB, is as follows: with the operating frequency and transmitter antenna size fixed, the oscillation amplitude is increased until the power incident at the receiver reaches the minimum value $P_{R,req}$ for successful demodulation, and the transmitter bias current at this point is recorded. This calculation takes into account variation of the oscillator linewidth with amplitude, and the effect of this linewidth variation on $P_{R,req}$. By repeating this process for different operating frequencies and antenna sizes, the minimum bias current, and the corresponding operating frequency that achieves it, can be determined as a function of maximum antenna size. The methods used are described in detail in the following sections.

The analysis in this paper extends that previously introduced by the authors. The optimisation trade-off presented in [10], which investigated the choice of preferred frequency, taking into account the antenna losses only, is completed by considering the circuit implementation. Deriving methods to analyse the cross-coupled oscillator, has enabled a comparison to be made with the Colpitts oscillator, which was considered in [11]. A far superior MOS model to that used in [11] has been developed to achieve more accurate results. The complete simulation method is presented here for the first time. The preferred frequency is plotted for two different data rates (1 Mb/s and 10 kb/s) allowing further important conclusions to be drawn.

A. Approach to Modelling

To evaluate the preferred transmission frequency for a given antenna constraint, the oscillator circuit must be accurately modelled. Normally circuit simulation is performed using highly advanced circuit simulators such as Spectre RF from Cadence Design Systems. Such a simulator is unfortunately not suited to this sort of global optimisation, since the range and number of variables is simply too large. Each specific set of parameters requires separate transient, periodic steady-state and periodic noise analyses to determine the oscillation voltage, the oscillation frequency and the corresponding phase noise. The transient method is time consuming since the circuit must reach its periodic steady-state, which requires a simulation time several orders of magnitude larger than the maximum time step [12]. Furthermore transient simulations normally require a certain amount of adjustment by the user to ensure start-up, making automation of such an optimisation process difficult. A custom simulation tool has therefore been implemented in MATLAB, which finds the necessary bias current for a given oscillation voltage amplitude, V_0, and calculates the oscillator line width. A transistor model has been developed which is based on EKV, whilst using some BSIM parameters and equations to increase accuracy.

II. Required Oscillation Amplitude

Successful demodulation demands a certain signal power, $P_{R,req}$, to be detected by the receiver, which in turn requires a certain power input to the transmitter antenna, $P_{T,req}$. This can be calculated using the Friis free space propagation formula [13], which has been shown to be accurate to within 10 dB for on-body communications [14]. For the case of the oscillator transmitter, the required transmit power determines a required oscillation voltage amplitude, $V_{0,req}$, which, using the Friis formula, is given by:

$$V_{0,req} = \sqrt{\frac{2R_{T,P}}{\eta_T \eta_R D_T D_R} \cdot \left(\frac{4\pi r}{\lambda_0}\right)^2 \cdot P_{R,req}} \qquad (1)$$

where the transmission distance is represented by r, the wavelength by λ_0; $\eta_{T(R)}$ and $D_{T(R)}$ represent the radiation efficiency and directivity for the transmitter (receiver) antenna respectively. $R_{T,P}$ is the total equivalent parallel resistance of the antenna at the oscillation frequency, ω_0.

A. Required Receive Power

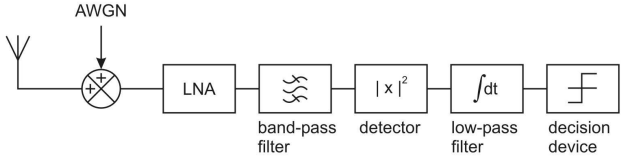

Fig. 1. Generic OOK receiver architecture.

For an incoming signal disturbed by additive white Gaussian thermal noise (AWGN) the required receive power, $P_{R,req}$ for successful demodulation is given by:

$$P_{R,req} = k \cdot T \cdot B \cdot SNR_{req} \cdot NF \qquad (2)$$

where k is Boltzmann's constant, T is the absolute temperature, and NF is the receiver noise figure. SNR_{req} is the input-referred signal to noise ratio required for a specified bit-error-rate (BER). SNR is taken as the ratio of the signal power to the noise power contained within the band B.

The value of SNR_{req} depends on the modulation/demodulation scheme and on the spectral purity of the carrier. The signal received from an oscillator transmitter, uncontrolled by a phase locked loop, will be disturbed by phase noise to an extent whereby the carrier linewidth cannot be assumed negligible compared to the data rate. In such a case the pre-detection bandwidth of the receiver has to be increased to contain the signal spectrally, and this inevitably leads to an increase in the noise power at the detector output. This problem has been studied extensively in the context of optical communications systems subject to laser phase noise. The results presented in [15] are used in this work in order to find the SNR_{req} for a particular ratio of carrier linewidth to the bit rate for the generic noncoherent OOK receiver shown in figure 1, assuming optimal pre-detection bandwidth and decision threshold. [15] uses the standard Lorentzian phase noise description and is thus applicable to the realm of RF oscillator transmitters if the contribution of flicker noise is neglected.

III. Variation of Oscillation Voltage with Bias Current

The relationship between the oscillation voltage amplitude, V_0, and the bias current, I_B, is required to calculate the necessary transmitter power dissipation for successful data transfer. The following is valid for the Colpitts oscillator in the limit $g_m/g_{mc} \to \infty$ [16]:

$$V_0 = \frac{2I_B}{g_{mc}} \tag{3}$$

where g_{mc} is the critical transconductance required for oscillation, g_m being the transconductance. In [16] a more generally valid expression for the oscillation voltage is found by multiplying the fundamental component of the drain current by the parallel tank resistance, $1/g_{mc}$. [17] finds the oscillation amplitude by solving the characteristic equation of the oscillator. The MOS transistor (MOST) is assumed to operate in either strong inversion saturation or cut-off in both [16] and [17]. [18] extends the analysis to include the strong inversion linear region, noting that the oscillation voltage amplitude would be overestimated for large voltages if this region were ignored.

For the cross-coupled oscillator in the current limited regime a simple approximation for the oscillation voltage amplitude is [19]:

$$V_0 = \frac{4}{\pi} \cdot I_B \cdot R_{P,eq} \tag{4}$$

At higher frequencies the current becomes almost sinusoidal, leading to the following approximation for V_0 [19]:

$$V_0 \approx I_B \cdot R_{P,eq} \tag{5}$$

Once again these equations are only asymptotic and are thus not suited to optimisation over a large parameter range. In [12] accurate periodic steady-state expressions are developed analytically for an nMOS cross-coupled oscillator, taking into account short-channel effects in the MOS strong inversion equations.

The models developed in [12], [16]–[18] are not directly suited to this work as they stand, primarily due to the MOS drain current model used. CMOS oscillators today usually use on-chip spiral inductors, which have a Q-factor of less than 10 [12], allowing strong inversion operation to be assumed and transistor output resistance to be ignored. Contrastingly, a high Q off-chip single-turn loop inductor is being considered in this work, requiring weak and moderate inversion to be included in the optimisation process. The MOS transistor output resistance must also be taken into account since the losses of the inductor may no longer dominate, especially for devices less than 0.5 μm in length.

In this section a new method for determining the required I_B to achieve a certain V_0 is developed, based on the principle of energy conservation. The method has the advantage of being completely independent of the MOS drain current model, allowing a more complete model to be easily used, and can be applied to both the Colpitts and cross-coupled oscillators.

A. Colpitts Oscillator

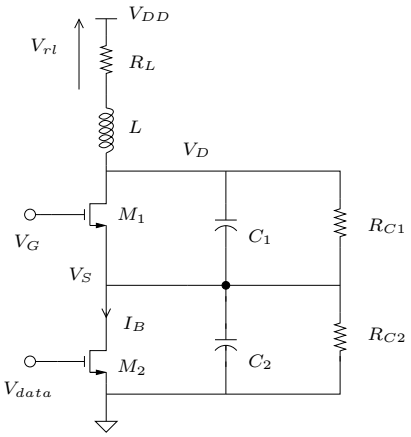

Fig. 2. Colpitts oscillator circuit.

Consider the Colpitts oscillator shown in figure 2. R_L is the series resistance of the inductor, L, whilst R_{C1} and R_{C2} represent the losses of the capacitors C_1 and C_2 at the oscillation frequency. Transistor $M2$ is used to switch the oscillator off and on in accordance with the OOK data to be transmitted. For this steady-state analysis transistor $M2$ is considered to act as a perfect current source of value I_B. Starting from the principle of the conservation of energy, the sum of the average power losses in the components must equal the total average power dissipation, $V_{DD} \cdot I_B$.

$$\begin{aligned} V_{DD}I_B &= \overline{V_S}I_B + \frac{1}{T_0}\int_0^{T_0} (V_D - V_S)\, I_{M1}(t)\, dt \\ &+ \frac{1}{T_0}\int_0^{T_0} V_{rl}^2 \cdot \frac{1}{R_{L,ac}} dt + \left(V_{DD} - \overline{V_D}\right) I_B \end{aligned} \tag{6}$$

$$+ \quad \frac{1}{T_0}\int_0^{T_0} \frac{(V_d - V_s)^2}{R_{C1}} dt$$
$$+ \quad \frac{1}{T_0}\int_0^{T_0} \frac{V_s^2}{R_{C2}} dt$$

where $I_{M1}(t)$ is the drain current of transistor M_1, which can be found if the four terminal voltages of the transistor are known at time, t. The gate voltage is set to a constant dc bias and the bulk is connected to ground. The drain and source voltages, V_D and V_S, are assumed to be given by:

$$V_D = \overline{V_D} + V_d \quad \text{where} \quad V_d = V_0 \cos(\omega_0 t) \tag{7}$$
$$V_S = \overline{V_S} + V_s \quad \text{where} \quad V_s = n_T V_0 \cos(\omega_0 t) \tag{8}$$

$\overline{V_D}$ and $\overline{V_S}$ are the average drain and source voltages respectively. V_0 is the oscillation voltage amplitude and n_T is the capacitive feedback ratio, given by:

$$n_T = \frac{C_1}{C_1 + C_2} \tag{9}$$

For a high Q tank the source and drain voltages can be taken as approximately sinusoidal and C_1 and C_2 can be considered to form an ideal capacitive divider [20].

V_{rl} is the ac voltage across the antenna resistance R_L, ac at the oscillation frequency ω_0. It is important to note that the antenna resistance is frequency dependent and therefore the dc value cannot be considered equal to the value at ω_0. The magnitude of V_{rl} is given by:

$$|V_{rl}| = \frac{R_{L,ac}}{\sqrt{R_{L,ac}^2 + \omega_0^2 L^2}} \cdot V_0 \tag{10}$$

Therefore the third term on the RHS of equation 6 becomes:

$$\frac{1}{T_0}\int_0^{T_0} V_{rl}^2 \cdot \frac{1}{R_{L,ac}} dt = \frac{R_{L,ac}}{R_{L,ac}^2 + \omega_0^2 L^2} \cdot \frac{V_0}{2} \tag{11}$$

The dc power dissipation due to $R_{L,dc}$ can be taken into account by the fourth term on the RHS of equation 6. In this work $\overline{V_D}$ is assumed to be equal to V_{DD} since the dc voltage drop across the inductor will be negligible. Since transistor M1 is the only dc path to ground, ignoring any capacitor leakage current, the following is true:

$$\frac{1}{T_0}\int_0^{T_0} I_{M1} dt = I_B \tag{12}$$

Using equations 7, 8 and 12, the second term on the RHS of equation 6 can be re-written as follows:

$$\begin{aligned}
&\frac{1}{T_0}\int_0^{T_0} (V_D - V_S) I_{M1} dt \\
&= \frac{\overline{V_D}}{T_0}\int_0^{T_0} I_{M1} dt - \frac{\overline{V_S}}{T_0}\int_0^{T_0} I_{M1} dt \\
&+ \frac{V_0(1-n_T)}{T_0}\int_0^{T_0} \cos(\omega_0 t) I_{M1} dt \qquad (13) \\
&= I_B\left(\overline{V_D} - \overline{V_S}\right) + \frac{V_0(1-n_T)}{T_0}\int_0^{T_0} \cos(\omega_0 t) I_{M1} dt
\end{aligned}$$

With simple manipulation, equation 6 reduces to the following:

$$-\frac{V_0^2}{2}\left[\frac{R_{L,ac}}{R_{L,ac}^2 + \omega_0^2 L} + \frac{(1-n_T)^2}{R_{C1}} + \frac{n_T^2}{R_{C2}}\right] = \frac{1}{T_0}(1-n_T) V_0 \int_0^{T_0} \cos(\omega_0 t) I_{M1} dt \tag{14}$$

The average source voltage, $\overline{V_S}$, that satisfies this energy conservation equation (14), can be found numerically or analytically depending on the MOST drain current model used. $\overline{V_S}$ is then inserted in equation 12 to obtain the required I_B for the given V_0.

B. Complementary Cross Coupled Differential Oscillator

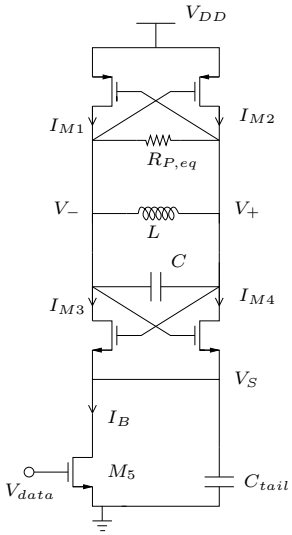

Fig. 3. Complimentary cross-coupled differential oscillator.

The same method is applied to the cross-coupled oscillator shown in figure 3. Transistor $M5$ is the equivalent of transistor $M2$ in the Colpitts oscillator and is considered to be a current source of value I_B. $R_{P,eq}$ represents the combined equivalent parallel resistance of the capacitor, C, and inductor, L. Note that the dc resistance of the inductor can be ignored in this case due to the inherent symmetry of the circuit. Assuming matched devices and a reasonable Q factor, the voltages V_+ and V_- can be expressed as follows:

$$V_+ = \overline{V_0} + \frac{V_0}{2}\cos(\omega_0 t) \tag{15}$$
$$V_- = \overline{V_0} - \frac{V_0}{2}\cos(\omega_0 t) \tag{16}$$

Again, applying the principle of energy conservation:

$$\begin{aligned}
V_{DD} I_B &= V_S I_B + \frac{V_0^2}{2R_{P,eq}} \qquad (17) \\
&+ \frac{1}{T_0}\int_0^{T_0} \left\{V_{DD} - \overline{V_0} + \frac{V_0}{2}\cos(\omega_0 t)\right\} I_{M1}\, dt \\
&+ \frac{1}{T_0}\int_0^{T_0} \left\{V_{DD} - \overline{V_0} - \frac{V_0}{2}\cos(\omega_0 t)\right\} I_{M2}\, dt
\end{aligned}$$

$$+ \quad \frac{1}{T_0}\int_0^{T_0}\left\{\overline{V_0} - \frac{V_0}{2}\cos(\omega_0 t) - V_S\right\} I_{M3}\, dt$$
$$+ \quad \frac{1}{T_0}\int_0^{T_0}\left\{\overline{V_0} + \frac{V_0}{2}\cos(\omega_0 t) - V_S\right\} I_{M4}\, dt$$

The current source node, V_S, is taken to be at dc since a tail capacitor C_{tail} is included in the circuit to significantly reduce the noise contribution of the tail current source as described in [21]. The symmetry (assuming good matching) of the circuit means that the bias current is equal to double the average current through each transistor:

$$I_B = \frac{2}{T_0}\int_0^{T_0} I_{Mk}\, dt \qquad \text{where k = 1, 2, 3 or 4} \qquad (18)$$

Furthermore, due to symmetry and the anti-phase nature of the two sides of the circuit, it can be seen that:

$$\frac{1}{T_0}\int_0^{T_0}\left\{V_{DD} - \overline{V_0} + \frac{V_0}{2}\cos(\omega_0 t)\right\}\cdot I_{M1}\, dt \qquad (19)$$
$$= \quad \frac{1}{T_0}\int_0^{T_0}\left\{V_{DD} - \overline{V_0} - \frac{V_0}{2}\cos(\omega_0 t)\right\}\cdot I_{M2}\, dt$$

and

$$\frac{1}{T_0}\int_0^{T_0}\left\{\overline{V_0} - \frac{V_0}{2}\cos(\omega_0 t) - V_S\right\}\cdot I_{M3}\, dt \qquad (20)$$
$$= \quad \frac{1}{T_0}\int_0^{T_0}\left\{\overline{V_0} + \frac{V_0}{2}\cos(\omega_0 t) - V_S\right\}\cdot I_{M4}\, dt$$

With a little simple manipulation equations 18, 19 and 20 are combined to give:

$$\frac{1}{T_0}\left[\int_0^{T_0}\cos(\omega_0 t)\cdot I_{M4}\, dt - \int_0^{T_0}\cos(\omega_0 t)\cdot I_{M2}\, dt\right] \qquad (21)$$
$$= -\frac{V_0}{2\cdot R_{P,eq}}$$

The two unknown dc points, $\overline{V_0}$ and V_S, that satisfy equations 18 and 21 simultaneously can be found numerically or analytically depending on the MOS transistor model. These allow the bias current to be evaluated for a given V_0.

IV. MOS Transistor Model

It is of increased importance to accurately model the MOS transistor for high Q oscillators, particularly at high frequencies where short channel devices are necessary. Weak and moderate inversion must be included in the analysis, the output resistance cannot be neglected, short channel effects should be modelled and high frequency limitations play an important role.

In this work the EKV (Enz Krummenacher Vittoz) model was used to model mobility reduction, short- and narrow-channel effects, channel length modulation, velocity saturation and charge-sharing using the equations presented in [22]. The model was improved using BSIM3v3 equations to model the substrate induced body effect and the parasitic source and drain resistances as described in [23]. The effective device dimensions were also modelled using BSIM3v3. It is important to consider the non-quasi-static (NQS) effect at RF frequencies. This was taken into account using the large signal NQS model presented in [24].

V. Transistor Sizing

In order to ascertain the minimum required bias current for a particular frequency and antenna size, an optimal transistor size must first be chosen. The factors to be considered are noise, oscillator loop gain and capacitance.

Transistor M1 in the Colpitts oscillator and transistors M1, M2, M3 and M4 in the cross-coupled oscillator are responsible for providing the loop gain needed for oscillation. A simple algorithm has been devised which searches for the optimal width-length combination for these transistors in order to provide the necessary start-up transconductance with the minimum bias current. The algorithm uses the small-signal NQS model presented in [25] to evaluate the transadmittance and takes into account the transistor output resistance and the losses of the tank components. The parasitic capacitance due to the MOS transistors must also be considered since this limits the maximum oscillation frequency for a given transistor size. Since the loop gain transistors conduct only at the point in the cycle at which the circuit is least sensitive to noise [26], and combined with the fact that a significant increase in phase noise still has a relatively small effect on the required SNR [15], noise can be ignored in the size optimisation of these transistors.

For the cross-coupled oscillator the nMOS devices should be matched as should the pMOS devices in order to achieve symmetrical operation. Furthermore, the devices are sized such that the transconductance of the pMOSTs will equal that of the nMOSTs since the $1/f^3$ phase noise corner frequency is improved through such a design [27].

The current source transistor should be sized for low noise performance.

VI. Phase Noise

The linewidth of the oscillator must be evaluated in order to determine the required SNR as detailed in section II-A. This analysis uses the theory developed by Hajimiri and Lee as detailed in [26], which is based on the conjecture that the amplitude and phase perturbations of an oscillator disturbed by noise are orthogonal. Although this assumption is not strictly valid [28] it yields accurate results in this case, since the oscillator is not perturbed by non-stationary sources [29]. Flicker noise has not been included in the phase noise analysis since the SNR dependence on linewidth presented in section II-A takes into account thermal noise only. The impulse sensitivity function (ISF) has been set to $-\sin\omega_0 t$, which corresponds to the ideal cosinusoidal oscillator [26]. A noise modulation function (NMF), $\alpha(\omega_0 t)$ is used to account for the cyclostationary nature of the channel thermal noise which varies periodically with the transistor operating point as described in [26]. The circuit noise models are based on those presented in [16] (Colpitts) and [30] (cross-coupled). The thermal noise contribution of each component was taken into account using models presented in [20], [31].

VII. Oscillator Model Evaluation

The energy conservation method, the MOS transistor model and the phase noise model presented above have been combined to form a complete steady-state oscillator simulation

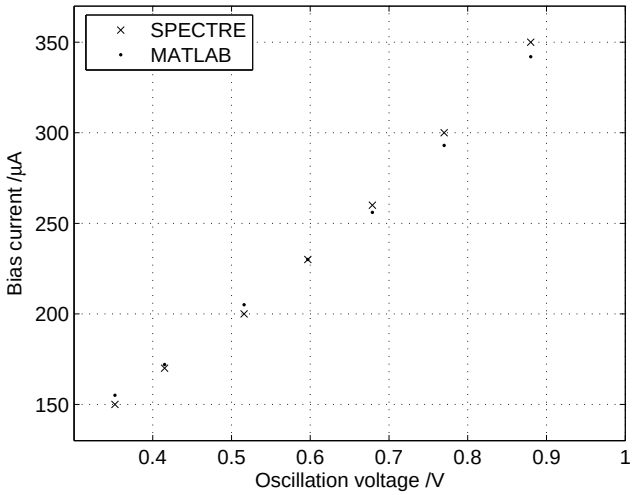

Fig. 4. Comparison of SPECTRE RF with MATLAB for oscillation voltage versus bias current characteristic of a 100 MHz cross-coupled oscillator (inductor of 1 nH with series resistance of 0.22 mΩ; transistor dimensions $W_{M1,2}$ = 20 μm, $L_{M1,2}$ = 400 nm, $W_{M3,4}$ = 15 μm, $L_{M3,4}$ = 600 nm).

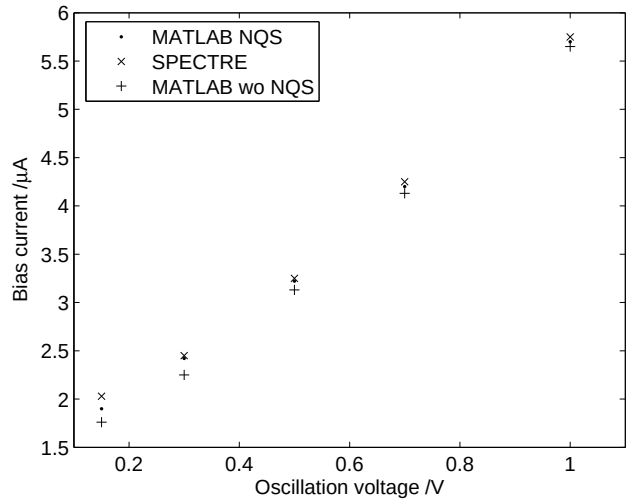

Fig. 5. Comparison of MATLAB required bias current predictions including and not including NQS with those from SPECTRE RF for a 2.5 GHz Colpitts oscillator (26.1 nH inductance with 1.37 Ω series resistance; transistor dimensions W_{M1} = 13 μm, L_{M1} = 400 nm).

tool. The accuracy of this tool has been evaluated through comparison with results from the SPECTRE RF simulator using the BSIM3 model. Figure 4 compares the bias current required for a certain oscillation voltage, predicted by both SPECTRE and MATLAB simulations for a 100 MHz complementary cross-coupled differential oscillator. Figure 5 makes the same comparison for a 2.5 GHz Colpitts oscillator, whilst also demonstrating the importance of taking into account the non-quasi-static effect at high frequency. Figures 4 and 5 show the close agreement between the custom MATLAB simulator and the industry standard SPECTRE RF simulator with BSIM3 MOS model.

VIII. Preferred Frequency

The methods and equations presented in the preceding sections have been combined with the loop antenna analysis of [10] to identify the preferred frequency in terms of minimal power consumption for a given constraint on transmitter antenna radius. The tank capacitors are assumed to have negligible losses in comparison to the antenna.

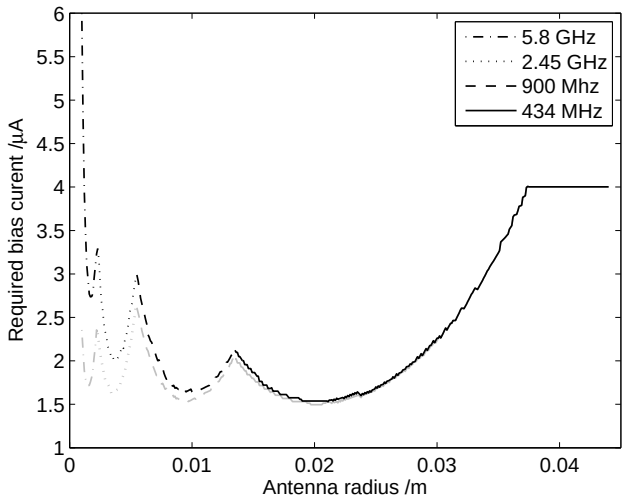

Fig. 6. Minimum Colpitts oscillator bias current required for successful demodulation against antenna radius for NF = 20 dB, r = 1 m. Grey line: data rate = 10kb/s. Black line: data rate = 1Mb/s.

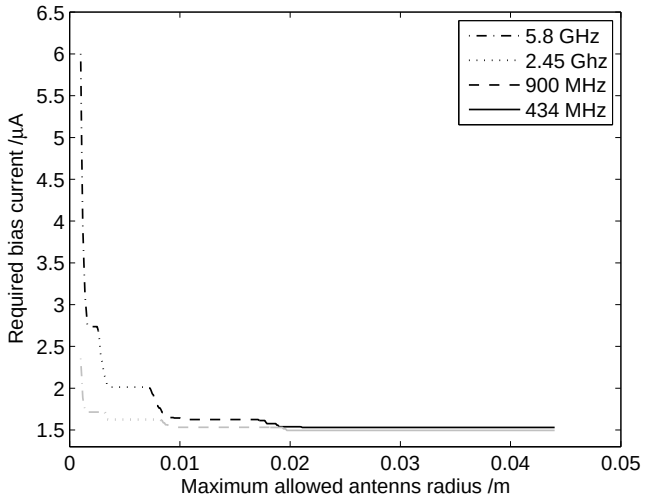

Fig. 7. Minimum Colpitts oscillator bias current required for successful demodulation against maximum allowed antenna radius for NF = 20 dB, r = 1 m. Grey line: data rate = 10kb/s. Black line: data rate = 1Mb/s.

Figures 6 and 7 show results from a Colpitts oscillator transmitter operated at 1.5 V supply, 0.8 V M1 gate bias voltage and capacitive feedback ratio n_T = 0.2. Figures VIII and 9 illustrate results from a complementary cross coupled differential oscillator transmitter operated at 1.5 V supply. For both oscillators, the required bias current is calculated for a

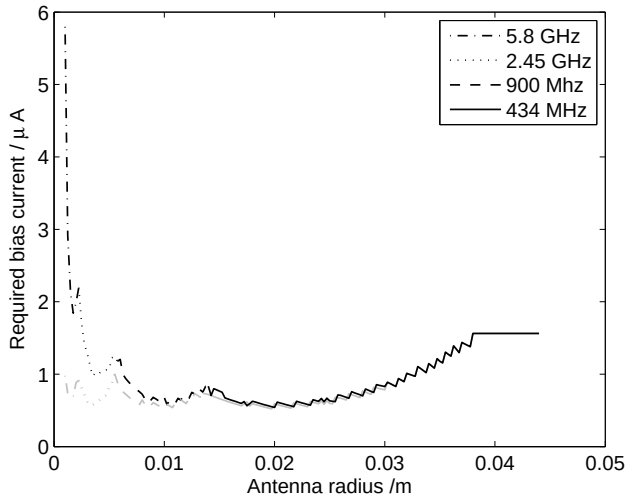

Fig. 8. Minimum cross-coupled oscillator bias current required for successful demodulation against antenna radius for NF = 20 dB, r = 1 m. Grey line: data rate = 10kb/s. Black line: data rate = 1Mb/s.

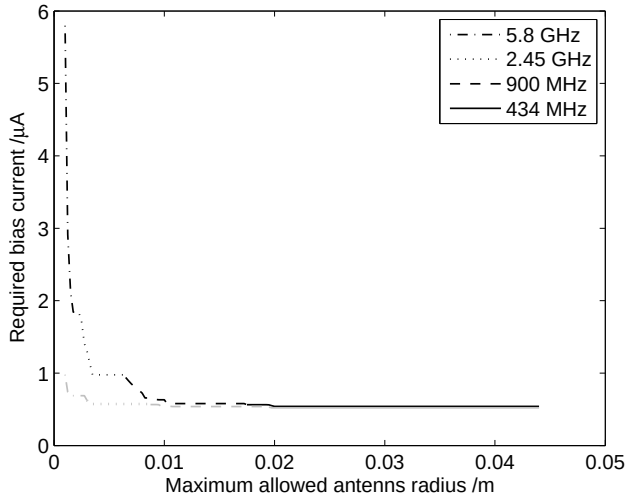

Fig. 9. Minimum cross-coupled oscillator bias current required for successful demodulation against maximum allowed antenna radius for NF = 20 dB, r = 1 m. Grey line: data rate = 10kb/s. Black line: data rate = 1Mb/s.

transmission distance of 1m, a receiver noise figure of 20 dB and a bit error rate of 10^{-9}. Figures 6 and VIII show the preferred frequency from among the ISM bands of 434 MHz, 900 MHz, 2.45 GHz and 5.8 GHz for a particular antenna radius for the data rates of 1 Mb/s and 10 kb/s as indicated in the figure caption. Figures 7 and 9 show the minimum required bias current for this preferred frequency as a function of the maximum allowed antenna radius.

A. Discussion

From figures 6 and VIII it can be seen that the required bias current for a particular frequency passes through a minimum at an antenna radius corresponding to an electrical size of about 0.2. For increasing antenna size, this optimal size is the point at which increasing antenna radiation efficiency is exactly balanced by the decreasing antenna Q-factor. The power consumption at this optimal electrical size decreases with frequency due to the improved power transfer and MOS transistor performance. Moving left to right in figures 7 and 9 the power consumption at any given preferred frequency falls with maximum allowed antenna size until the optimal size for that frequency is reached. Thereafter, antenna size and power consumption remain fixed until the next preferred frequency boundary is reached, since the required bias current cannot be reduced through increasing the antenna size beyond its optimum value. The transition to the next ISM band occurs when the disadvantages of no longer being at the optimal antenna size are exactly compensated by the improvements in MOS performance and power transfer offered by the lower frequency.

Figures 7 and 9 show that, for the higher frequencies of 5.8 GHz and 2.45 GHz, a transmitter operating at the lower data rate (10 kb/s) consumes significantly less power than one operating at the higher data rate (1 Mb/s). This applies to both the Colpitts and cross-coupled oscillators. In contrast, changing the data rate has little effect on the power consumption of either type of oscillator at the lower frequencies. This behaviour can be explained with the aid of figure 10, which shows the typical form for the variation in bias current with oscillation amplitude. Neglecting the effect of the the signal linewidth on SNR_{req}, the required oscillation amplitude at the transmitter is expected to be proportional to the square root of the data rate at any given frequency (see equations 1 and 2 in Section II). Thus a hundred-fold reduction in the data rate should allow a tenfold reduction in the oscillation amplitude. However, as can be seen from equation 1, the required oscillation amplitude is also inversely proportional to the wavelength, so that lower amplitudes are required at lower frequencies. For the links modelled in this paper, the amplitudes at 434 MHz and 900 MHz are sufficiently small ($<$0.05 V) that they lie in the region of figure 10 where the bias current shows only weak dependence on the oscillation amplitude. In contrast, the amplitudes at 2.45 GHz and 5.8 GHz lie on the steeper part of the graph where changing the oscillation amplitude has a noticeable effect on the bias current.

In a real system it is often desirable to include some form of frequency control, in which case a tunable capacitor would be necessary. A. S. Porret et al have shown in [32] that high Q-factor varactors are possible in a standard digital CMOS process. Another option is to use high-Q RF MEMS capacitors such as those presented in [33]. Another possibility to reduce the impact of any low-Q tunable element would be use it as capacitor C_2 in the Colpitts oscillator, since the parallel resistance of the tunable capacitor would be multiplied by $1/n_T^2$ when considered as an equivalent parallel resistance across the tank. However, it may well be the case that tunable capacitors will limit the Q-factor, in which case the analysis and models already developed can be easily applied to find a modified preferred frequency, taking into account the variation of capacitor Q with frequency.

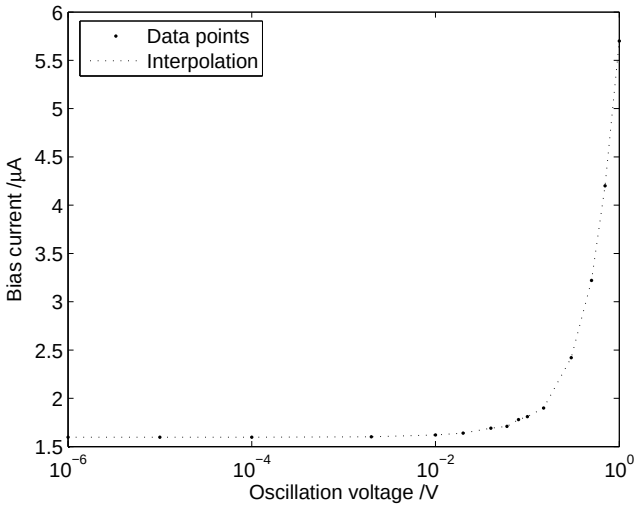

Fig. 10. Required bias current versus oscillation amplitude for the 2.5 GHz Colpitts oscillator used for figure 5.

IX. Conclusion

We have developed a method for determining the preferred carrier frequency for simple oscillator transmitters for which the antenna is size-constrained. To do this a new periodic steady-state simulation method has been developed along with an accurate MOST model. Unlike other methods, this new approach is particularly suited to global optimisation. It is shown that, by carefully choosing the frequency and by sizing the antenna accordingly, it is possible to achieve 1 Mb/s over a 1m wireless link with a transmitter power consumption of less than 10 μ W.

Comparison of figure 7 with figure 9 demonstrates that for the same performance the cross-coupled oscillator consumes less power than the Colpitts oscillator. This is essentially because the Colpitts oscillator feeds back only the fraction, n_T, of the tank voltage, V_0, whereas the complementary cross-coupled differential oscillator feeds back the entire tank voltage. This means that a lower transconductance and hence bias current is required for the cross-coupled oscillator to achieve the same V_0.

It can be further concluded that for any of the frequencies it is far more power efficient to use the oscillator transmitter at a higher data rate than required. In this way the transmitter can be operated at a low duty cycle whilst still achieving the necessary data rate. Such a method of power reduction could be limited by the available bandwidth, the start-up time of the oscillator, and the need for data storage until transmission.

References

[1] Guang-Zhong Yang (Ed.), *Body Sensor Networks*, Springer-Verlag, London 2006.

[2] P. D. Mitcheson, D. C. Yates, E. M. Yeatman, T. C. Green and A. S. Holmes, "Modelling for optimisation of self-powered wireless sensor nodes," *International Workshop on Wearable and Implantable Body Sensor Networks*, IEE Proceedings, pp 53-57, April 2005.

[3] J.A. Paradiso, T. Starner, "Energy scavenging for mobile and wireless electronics," *IEEE Pervasive Computing Magazine*, vol. 4, pp. 18-27, January-March 2005.

[4] B. Ziaie, K. Najafi and D.J Anderson, "A low-power miniature transmitter using a low-loss silicon platform for biotelemetry," *IEEE Proceedings of the Engineering in Medicine and Biology Society*, 19^{th} international conference, vol. 5, pp. 2221 - 2224, 1997.

[5] M. Suster, W.H. Ko, D.J. Young, "An optically powered wireless telemetry module for high-temperature MEMS sensing and communication," *IEEE Journal of Microelectromechanical Systems*, vol. 13, no. 3, pp. 536-541, June 2004.

[6] M. Sasaki, "Design of a Millimeter-Wave CMOS Radiation Oscillator With an Above-Chip Patch Antenna," *IEEE Transactions on Circuits and Systems II: Express Briefs*, vol. 53, no. 10, pp. 1128-1132, Oct. 2006.

[7] N. Joehl, C. Dehollain, P. Favre, P.Deval and M. Declercq, "A Low-power 1GHz Super-Regenerative Transceiver with Time-Shared PLL Control," *IEEE Journal of Solid-State Circuits*, vol. 36, no. 7, pp. 1025-1031, July 2001.

[8] B. Otis, Y.H. Chee, J. Rabaey, "A 400 W-RX, 1.6 mW-TX super-regenerative transceiver for wireless sensor networks," *Proc. IEEE Solid-State Circuits Conf.*, vol. 1, pp. 396-397, 2005.

[9] Y. H. Chee, A. M. Niknejad, J. M. Rabaey, "An Ultra-Low-Power Injection Locked Transmitter for Wireless Sensor Networks,"*IEEE Journal of Solid-State Circuits*, vol.41, no.8, pp. 1740-1748, August 2006.

[10] D. C. Yates, A. S. Holmes and A. J. Burdett, "Optimal transmission frequency for ultra-low power short-range radio links,", *IEEE Trans. Circuits and Systems - I*, vol. 51, no. 7, pp. 1405-1413, July 2004.

[11] D.C. Yates and A.S. Holmes, "Loop antenna design for ultra low power transmitter," *IEEE International Workshop on Antenna Technology: Smart Antennas and Novel Metamaterials*, pp. 287 - 290, Singapore, 7-9 March 2005.

[12] M. M. Mansour and A. Mehrotra, "Analysis techniques for obtaining the steady-state solution of MOS LC oscillators," *Proceedings of the 2004 International Symposium on Circuits and Systems*, vol. 5 pp. 512-515, May 2004.

[13] C. A. Balanis, *Antenna Theory, Analysis and Design*, Second Edition, New York: Wiley 1997.

[14] M. R. Kamarudin, Y. I. Nechayev, P. S. Hall, "Antennas for on-body communication systems," *IEEE International Workshop on Antenna Technology: Small Antennas and Novel Metamaterials*, pp. 17-20, 7-9 March 2005.

[15] G. Einarsson, J. Strandberg and I. T. Monroy, "Error probability evaluation of optical systems disturbed by phase noise and additive noise," *Journal of Lightwave Technology*, vol. 13, no. 9, pp 1847-1852, September 1995.

[16] Q. Huang, "Phase noise to carrier ratio in LC oscillator," *IEEE Transactions on Circuits and Systems Part I*, vol. 47, no. 7 , pp. 965 - 980, July 2000.

[17] I. M. Filanovsky, C. J. M. Verhoeven and M. Reja, "Remarks on Analysis, Design and Amplitude Stability of MOS Colpitts Oscillator," *IEEE Transactions on Circuits and Systems II: Express Briefs*, vol. 54, no.9, pp.800-804, Sept. 2007.

[18] K. Mayaram, "Output voltage analysis for the MOS Colpitts oscillator," *IEEE Transactions on Circuits and Systems I: Fundamental Theory and Applications*, vol. 47, no. 2, pp. 260-263, February 2000.

[19] A. Hajimiri and T. H. Lee, "Design issues in CMOS differential oscillators," *IEEE Journal of Solid-State Circuits*, vol. 34, no. 5, pp 717-724, May 1999.

[20] T. H. Lee, *The Design of CMOS Radio-Frequency Integrated Circuits*, Cambridge University Press 1998.

[21] D. Ham and A. Hajimiri, "Concepts and methods in optimization of integrated LC VCOs," *IEEE Journal of Solid State Circuits*, vol. 36, no. 6, pp. 896-909, June 2001.

[22] M. Bucher et. al. *The EPFL-EKV MOSFET Model Equations for Simulation*, Technical Report, Model Version 2.6, June, 1997, Revision I, September, 1997, Revision II, July, 1998, Electronic Laboratories, Swiss Federal Institute of Technology (EPFL), Lausanne, Switzerland, obtained from http://legwww.epfl.ch/ekv/pdf/ekv_v262.pdf

[23] W. Liu et. al., *BSIM3v3.2.2 MOSFET Model Users' Manual*, University of California, Berkeley, 1999.

[24] M. Chan, K. Y. Hui, C. Hu, P. K. Ko, "A robust and physical BSIM3 non-quasi-static transient and AC small-signal model for circuit simulation," *IEEE Transactions on Electron Devices*, vol. 45, No. 4, pp. 834-841, April 1998.

[25] C. C. Enz, "A MOS transistor model for RF IC design valid in all regions of operation," *IEEE Trans. on Microwave Theory and Techniques*, vol. 50, no. 1, pp. 342 - 359, Jan 2002.

[26] A. Hajimiri and T. H. Lee, "A general theory of phase noise in electrical oscillators," *IEEE Journal of Solid-State Circuits*, vol. 33, no. 2, pp. 179-194, February 1998.
[27] M. del M. Mershensen, A. Hajimiri, S. S. Mojan, S. P. Boyd and T. H. Lee, "Design and optimization of LC oscillators," *1999 IEEE/ACM International Conference on Computer-Aided Design*, Digest of Technical Papers, pp 65 - 69, 7-11 November 1999.
[28] A. Demir, A. Mehrotra, J. Roychowdhury, "Phase noise in oscillators: a unifying theory and numerical methods for characterization," *IEEE Trans. Circuits and Systems I: Fundamental Theory and Applications*, vol. 47, iss. 5, pp. 655-674, May 2000.
[29] P. Vanassche, G. Gielen, Willy Sansen, "On the difference between two widely publicized methods for analyzing oscillator phase behavior," *2002 IEEE/ACM International Conference on Computer Aided Design*, pp. 229-233, 2002.
[30] A. Hajimiri and T. H. Lee, "Phase noise in CMOS differential LC oscillators," *Proc. VLSI Circuits*, pp 69-71, June 1998.
[31] C. C. Enz, F. Krummenacher and E. A. Vittoz, "An analytical MOS transistor model valid in all regions of operation and dedicated to low-voltage and low-current applications," *Analog Integrated Circuits and Signal Processing, Kluwer Academic Publishers*, pp. 83-114, July 1995.
[32] A.-S. Porret, T. Melly, C. C. Enz and E. A. Vittoz, "Design of high-Q varactors for low-power wireless applications using a standard CMOS process," *IEEE Journal of Solid-State Circuits*, vol. 35, no. 3, pp. 337-345, March 2000.
[33] T.G.S.M. Rijks, J.T.M. van Beek, P.G. Steeneken, M.J.E. Ulenaers, J. De Coster, R. Puers, "RF MEMS tunable capacitors with large tuning ratio," *17th IEEE International Conference on Micro Electro Mechanical Systems (MEMS)* pp. 777-780, 2004.